ELSEVIER

Journal of Molecular Catalysis 91 (1994) 7–17

JOURNAL OF MOLECULAR CATALYSIS

Stereoselective oxidation of enantiomeric amines by a monoamine oxidase model of chiral iron(III) porphyrins

Katsutoshi Ohkubo*, Takashi Sagawa, Yoshihiro Minamoto

Department of Applied Chemistry, Faculty of Engineering, Kumamoto University, Kurokami, Kumamoto 860 Japan

(Received June 10, 1993; accepted January 17, 1994)

Abstract

The stereoselective oxidation of enantiomeric amines (*R*(+)- or *S*(−)-α-phenylethylamine, **2a** or **2b**) has been performed with the chiral iron(III) porphyrin complexes of 5,10,15,20-tetrakis[*p*-((−)-menthylcarbamoyl)phenyl]porphyrin ($Fe^{III}ClT_{men}PP$, **1a**) and α,α,α,α-isomer of 5,10,15,20-tetrakis[*o*-((*t*-butyloxycarbonyl)-L(−)-alaninamino)phenyl]porphyrinato iron(III) chloride ($Fe^{III}ClT_{boc-Ala}PP$, **1b**) in benzene at 25°C. The reaction obeyed biphasic kinetics, and **1a** showed higher activity and stereoselectivity rather than **1b**. On the basis of the kinetic analysis of the racemic amine oxidation by *meso*-tetraphenylporphyrinato iron(III) chloride ($Fe^{III}ClTPP$, **1c**), the stereoselective molecular recognition of the enantiomeric **2a–b** substrates by **1a** or **1b** was found in the ligation step for the formation of the bis-ligated $Fe^{III}(amine)_2$ complex (**4**) and in the reduction of the chiral complex of **4** to the iron(II) one (**3**) by **2a** (not predominant) or **2b** (predominant) in the outer-sphere contact region of the chiral complex; the extent of the stereoselection by **1a** (possessing the chiral portion in the equatorial position for the porphyrin plane) or **1b** (possessing the chiral portion in the axial position for the porphyrin plane) was higher in the reduction step or in the second ligation step, respectively.

Keywords: Chiral complexes; Iron; Monoamine oxidase; Oxidation; Porphyrin complexes; Stereoselectivity

1. Introduction

Hemeproteins exhibit a site specific activity for the recognition of their substrates by controlling the secondary structures of poly(amino acids) which is proximal to the heme

*Corresponding author; tel. (+81-96)3442111, fax. (+81-96)3451576.

SSDI 0304-5102(94)00020-V

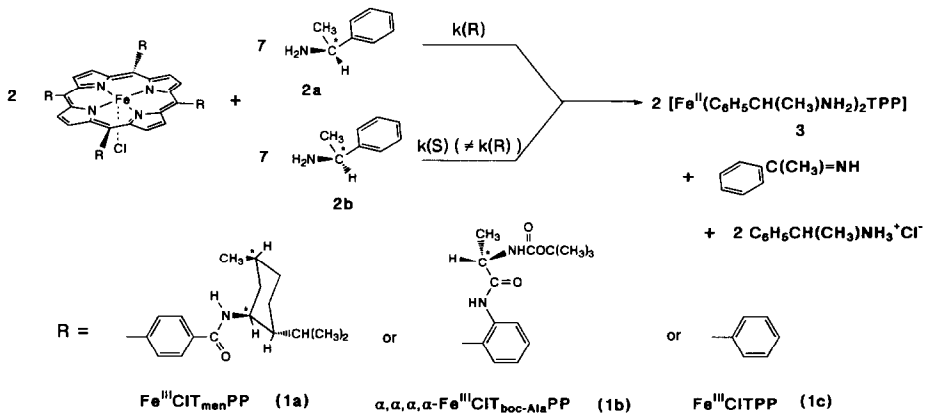

Scheme 1.

(iron complex of protoporphyrin IX). Such a specific site consists of the amino acid residues which behave as the ligands of the central iron and as the functional field in close contact to the porphyrin ring. It has often been postulated that the circumstances around the heme play an important role in the enzymatic function of the hemeprotein by controlling the cavity size and the reaction field for the recognition and activation of the specific substrates [1]. In this respect, the host–guest reactions with the hemeprotein–model metalloporphyrins have recently appeared in the investigations of the substrate recognition (including the stereoselective one) of such organic substrates as amines [2], amino acids [3], enantiomeric amino acid esters [4], and chiral phosphines [5] by metalloporphyrins. However, there is no report dealing with stereoselective hemeprotein-like reactions except for the stereoselective epoxidation with the cytochrome P-450 models [6]. We report here the first stereoselective monoamine oxidase reaction in the following reaction of *R*(+)- or *S*(−)-α-phenylethylamine (**2a** or **2b**) and chiral iron(III) porphyrin complexes of 5,10,15,20-tetrakis[*p*-((−)-menthylcarbamoyl)phenyl]porphyrin ($Fe^{III}ClT_{men}PP$, **1a**) and α,α,α,α-isomer of 5,10,15,20-tetrakis[*o*-((*t*-butyloxycarbonyl)-L(−)-alaninamino)-phenyl]-porphyrinato iron(III) chloride ($Fe^{III}ClT_{boc-Ala}PP$, **1b**). (See Scheme 1.)

The present work was performed for the extension of the previous amine oxidation by the achiral iron(III) porphyrins [7,8].

2. Experimental

2.1. Materials

Benzene was washed successively with concentrated sulfuric acid, water, sodium hydroxide, and water. Then the organic solvent was dried over calcium chloride, dried again, and distilled from Na before use. All other chemical reagents used were of reagent grade. Synthesis of tetraphenylporphyrin free base (H_2TPP) is based on the method described by

Adler and co-workers [9]. The preparation of metalloporphyrins containing iron were carried out according to the literature [10].

2.2. Preparation of iron(III) complexes of chiral porphyrins

5,10,15,20-Tetrakis[*p*-((−)-menthylcarbamoyl)phenyl]porphyrin free base ($H_2T_{men}PP$) and the $\alpha,\alpha,\alpha,\alpha$-isomer of 5,10,15,20-tetrakis[*o*-((*t*-butyloxycarbonyl)-L(−)-alaninamino)phenyl]porphyrin free base ($H_2T_{boc-Ala}PP$) were prepared as described previously [11]. 5,10,15,20-Tetrakis[*p*-((−)-menthylcarbamoyl)phenyl]porphyrinato iron(III) chloride ($Fe^{III}ClT_{men}PP$, **1a**) was prepared as follows: 0.2 g (0.15 mmol) of $H_2T_{men}PP$, 0.1 g (1.2 mmol) of sodium acetate, and 0.1 g (0.62 mmol) of iron(III) chloride were dispersed in acetic acid (50 cm^3). Then the mixtures were refluxed for 2 h and were cooled to room temperature. The addition of *n*-hexane to the above mixtures resulted in the precipitates of **1a**. The crude crystals of the complex were purified by washing them with acetic acid and water and were recrystallized from $CHCl_3$–*n*-hexane to afford 0.18 g (84%) of pure $Fe^{III}ClT_{men}PP$. UV (benzene): λ_{max} 507 nm (ϵ 8600 $dm^3 \cdot mol^{-1} \cdot cm^{-1}$), 570 (3200), 657 (2200), 684 (2300). Anal. Calcd for $C_{88}H_{120}N_8O_{12}FeCl$: C, 67.18; H, 7.69; N, 7.12%. Found: C, 67.22; H, 7.30; N, 7.58%. The $\alpha,\alpha,\alpha,\alpha$-isomer of 5,10,15,20-tetrakis[*o*-((*t*-butyloxycarbonyl)-L(−)-alaninamino)phenyl]porphyrinato iron(III) chloride ($Fe_{III}ClT_{boc-Ala}PP$, **1b**) was prepared as follows: 0.1 g (0.073 mmol) of $H_2T_{boc-Ala}PP$, 0.4 cm^3 of 2,6-lutidine, and 0.1 g (0.62 mmol) of iron(III) chloride were dissolved in THF (30 cm^3). The mixtures were then refluxed for 2 h and were evaporated to dryness before dissolving them in *n*-hexane. The hexane solution was then cooled to room temperature to obtain the precipitates of **1b**, and the crude product was washed with water and petroleum ether. Recrystallization from $CHCl_3$–*n*-hexane gave 0.098 g (92%) of **1b**. UV (benzene): λ_{max} 508 nm (ϵ 13400 $dm^3 \cdot mol^{-1} \cdot cm^{-1}$), 579 (4500), 647 (4200). Anal. Calcd for $C_{76}H_{92}N_{12}O_{16}FeCl$: C, 60.02; H, 6.10; N, 11.05%. Found: C, 60.10; H, 5.55; N, 10.76%.

2.3. ESR measurement

ESR spectra of the mixed system of **1c** and **2a–b** in CH_2Cl_2 were recorded in the frozen state at −196°C with a JEOL spectrometer (MgO powder doped with Mn^{II} were used as a standard with 100 kHz field modulation).

2.4. Reaction procedures

The oxidation of 4.0 cm^3 **2a** or **2b** (3.1×10^{-2} mol) by 5.0×10^{-5} mol of **1a**, **1b**, or **1c** were carried out for 4 h in 4.0 cm^3 benzene in N_2. The product of the imine was hydrolyzed to acetophenone and was analyzed by using Hitachi gas chromatograph 063 equipped with PEG 15%–Uniport B 60/80 (3 mm × 2 m) column (retention time of 9.83 min at 120°C).

3. Results and discussion

*3.1. Spectrophotometric measurement of an achiral iron(III) porphyrin complex (**1c**) in the reaction system*

Addition of racemic **2a–b** to *meso*-tetraphenylporphyrinato iron(III) chloride (**1c**) in benzene under N_2 at 25°C, resulted in the changes of the electronic spectra of **1c** as shown in Fig. 1.

The disappearance of the charge-transfer (from Cl to Fe(III)) band in **1c** at 650 nm [12] with the formation of the new band at 550 nm indicates that the **2a–b** coordinates to **1c** so as to form bis-ligated $[Fe^{III}(amine)_2TPP]^+Cl^-$ (**4**). There is no isosbestic point in Fig. 1 so that the amines can reduce **1c** to $Fe^{II}(amine)_2TPP$ (**3**) after the formation of **4**. Therefore, the oxidation of amine substrates by **1c** proceeds via the elementary steps shown in Scheme 2.

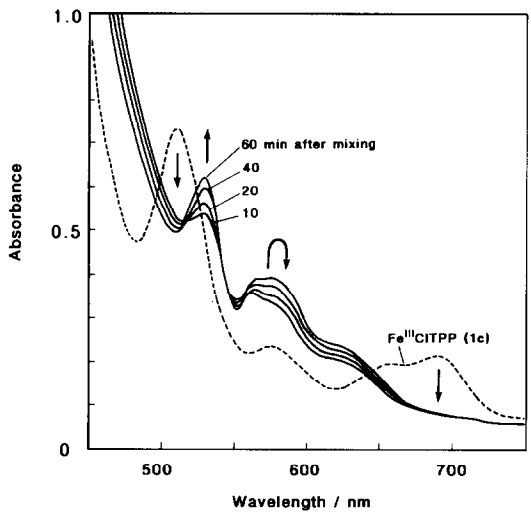

Fig. 1. The visible spectra for the oxidation of **2a–b** (2.0 mol dm^{-3}) by **1c** (5.0×10^{-5} mol dm^{-3}) in benzene at 25°C.

$$\mathbf{1c} + \mathbf{2a\text{-}b} \underset{k_{-1}}{\overset{k_1}{\rightleftharpoons}} \underset{\mathbf{4'}}{Fe^{III}(C_6H_5CH(CH_3)NH_2)ClTPP} \qquad (2a)$$

$$\mathbf{4'} + \mathbf{2a\text{-}b} \underset{k_{-2}}{\overset{k_2}{\rightleftharpoons}} \underset{\mathbf{4}}{[Fe^{III}(C_6H_5CH(CH_3)NH_2)_2TPP]^+Cl^-} \qquad (2b)$$

$$\mathbf{4} + \mathbf{2a\text{-}b} \xrightarrow{k_3} \underset{\mathbf{3}}{Fe^{II}(C_6H_5CH(CH_3)NH_2)_2TPP} + C_6H_5\dot{C}H(CH_3)\overset{+\cdot}{N}H_2 + Cl^- \qquad (2c)$$

Scheme 2.

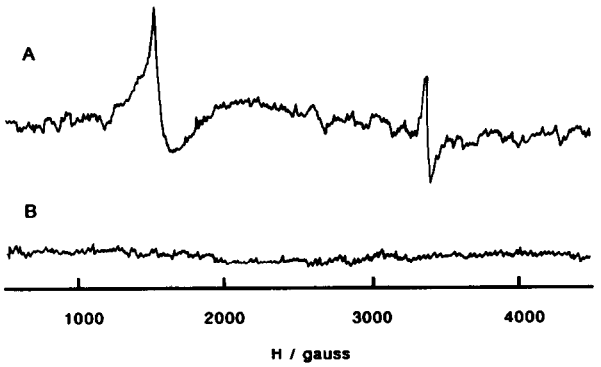

Fig. 2. ESR spectra of **1c** (0.5 mmol dm^{-3}) in the presence of **2a–b** (2.0 mol dm^{-3}) in CH_2Cl_2.

In this regard, the ESR spectrum observed for the mixture of **1c** taking a high spin state (5/2) [8] and excess **2a–b** in CH_2Cl_2 at −196°C showed two signals at $g=2$ and 6 just after mixing them (Fig. 2A).

These two signals may be assigned to the high spin (5/2) five-coordinated iron(III) porphyrin complex [8] of $[Fe^{III}(C_6H_5CH(CH_3)NH_2)TPP]^+Cl^-$ or the mixture, $g=6$ for $Fe^{III}ClTPP$ and $g=2$ for an organic radical. When the reaction mixture was stirred for several hours at 25°C, the two signals at $g=2$ and 6 disappeared (Fig. 2B) which presumably indicates the reduction of **4** to **3** (spin state 0 [13]) by the amine, though the formation of the low spin (1/2) six-coordinated iron(III) porphyrin complex of **4** has not been confirmed.

*3.2. Kinetics of ligation and oxidation steps of racemic α-phenylethylamine (**2a–b**)*

The overall rate constants (k^{obs}) for the reactions in Scheme 2 were determined spectrophotometrically by monitoring the absorbance (A) at $\lambda_{max}=528$ nm, and the present reactions obeyed the pseudo-first-order rate law:

$$k^{obs}t=\ln[(A_\infty-A_0)/(A_\infty-A_t)]=\ln[\mathbf{1c}]_0/[\mathbf{1c}]$$

where A_∞ = the end point of the absorbance at 528 nm, A_0 = the initial absorbance at 528 nm, A_t = the absorbance at an arbitrary reaction time (t) at 528 nm, $[\mathbf{1c}]_0$ = the initial concentration of **1c**, and $[\mathbf{1c}]=[\mathbf{1c}]_0-([\mathbf{4'}]+[\mathbf{4}]+[\mathbf{3}])$. Although this kinetic relation is plausible as shown in Fig. 3, it can be seen from Fig. 3 that the present reaction is biphasic, and the rate constants (slopes of k_1^{obs} and k_2^{obs}) clearly increase with increasing initial concentration of **2a–b**; The k_1^{obs} and k_2^{obs} values are listed in Table 1.

The k_1^{obs} value which is mainly dependent on the relatively slow Reaction (2b) is decreased to be the k_2^{obs} one by the participation of the second slow reaction (viz. Reaction (2c)) in the amine oxidation; in Reaction (2c), the third free ligand (**2a** or **2b**) is can cause an electron transfer to the porphyrin periphery in the contact outer-sphere of **4**, and the subsequent dissociation of the outer-sphere adduct would yield **3** as shown by Reaction (2c') in Scheme 3.

Then, the reaction rate (R) of amine oxidation by **1c** is evaluated by Eq. 1.

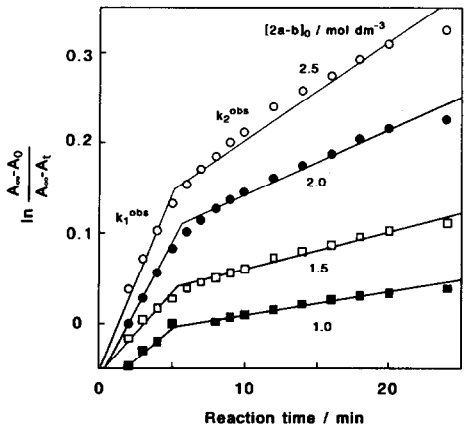

Fig. 3. Pseudo-first-order plots for the oxidation of **2a–b** (1.0, 1.5, 2.0 and 2.5 mol dm^{-3}) by **1c** (5.0×10^{-5} mol dm^{-3}) in benzene at 25°C.

Table 1
Pseudo-first-order rate constants for the oxidation of **2a** (or **2b**) by **1c** in benzene at 25°C[a]

[**2a**(or **2b**)]$_0$	$10^4 k_1^{obs}$	$10^4 k_2^{obs}$
mol·dm^{-3}	s^{-1}	s^{-1}
1.0	2.44	0.44
1.5	2.49	0.82
2.0	4.62	1.33
2.5	5.23	1.84

[a] [**1c**] $=5.0\times10^{-5}$ mol·dm^{-3}

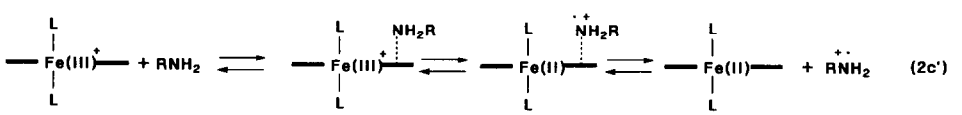

Scheme 3.

$$R = k_2^{obs}[\mathbf{1c}] = d[\mathbf{3}]/dt \quad (1)$$

The generated aminium cation radical readily converts to imine (only one product) via Reaction (3a–c) in Scheme 4; the imine was identified as acetophenone, obtained by the hydrolysis of the imine, and more than 90% yield of **3** from **1c** was observed in the amine oxidation for 20 min.

The plausibility of the proposed mechanism is then appraised on the basis of the kinetic analysis. From Schemes 2 and 4, a stationary state assumption for the concentrations of the reaction intermediates, $d[\mathbf{4}]/dt = d[\mathbf{4'}]/dt = d[>CHNH_2]/dt = d[>CNH_2]/dt = d[>CNH_2]/dt = 0$, gave Eq. 2.

$$>\dot{\overset{+}{C}}HNH_2 + Cl^- + RNH_2 \xrightarrow{k_4} >\dot{C}NH_2 + RNH_3^+Cl^- \quad (3a)$$

$$>\dot{C}NH_2 + [Fe^{III}(RNH_2)_2TPP]^+Cl^- \xrightarrow{k_5} >\overset{+}{C}NH_2 + Fe^{II}(RNH_2)_2TPP + Cl^- \quad (3b)$$

$$>\overset{+}{C}NH_2 + Cl^- + RNH_2 \xrightarrow{k_6} >C{=}NH + RNH_3^+Cl^- \quad (3c)$$

Scheme 4.

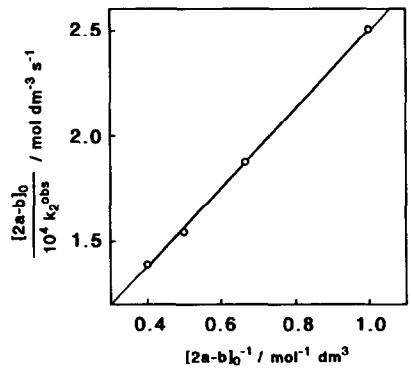

Fig. 4. Linear kinetic relation between $[\mathbf{2a–b}]_0/k_2^{obs}$ and $[\mathbf{2a–b}]_0^{-1}$.

$$\frac{d[\mathbf{3}]}{dt} = k_3[\mathbf{4}][\mathbf{2a–b}] + k_5[\mathbf{4}][>\dot{C}NH_2]$$

$$= \frac{2k_1k_2k_3[\mathbf{2a–b}]^3[\mathbf{1c}]}{k_{-1}k_{-2} + 2k_{-1}k_3[\mathbf{2a–b}] + 2k_2k_3[\mathbf{2a–b}]^2} \quad (2)$$

From Eqs. 1 and 2, k_2^{obs} can be given as:

$$k_2^{obs} = \frac{2k_1k_2k_3[\mathbf{2a–b}]^3}{k_{-1}k_{-2} + 2k_{-1}k_3[\mathbf{2a–b}] + 2k_2k_3[\mathbf{2a–b}]^2} \quad (3a)$$

Since the product of the rate constants ($k_{-1}k_{-2}$) is small compared with the other terms in Eq. 3a, the rate constant k_2^{obs} can be represented as Eq. 3b, which is rewritten as Eq. 3c:

$$k_2^{obs} = \frac{k_1k_2[\mathbf{2a–b}]^2}{k_{-1} + k_2[\mathbf{2a–b}]} \quad (3b)$$

$$\frac{[\mathbf{2a–b}]}{k_2^{obs}} = \frac{k_{-1}}{k_1k_2}\frac{1}{[\mathbf{2a–b}]} + \frac{1}{k_1} \quad (3c)$$

The linear relation between $[\mathbf{2a–b}]_0/k_2^{obs}$ and $[\mathbf{2a–b}]_0^{-1}$ in Eq. 3c was confirmed by using the k_2^{obs} values (in Table 1) as illustrated in Fig. 4.

From Fig. 4, the values of k_1 and k_{-1}/k_2 were obtained to be 1.6×10^{-6} dm$^3\cdot$mol$^{-1}\cdot$s^{-1} and 3.1×10^{-2} mol$\cdot$dm^{-3} respectively. The temperature dependence of the k_2^{obs} values was also examined for the present oxidation of **2a–b** by **1c**; The oxidation reaction in the temperature range of 298–318 K resulted in the activation parameters of $\Delta H^{\neq}=2.69$ kJ$\cdot$mol^{-1} and $\Delta S^{\neq}=-310.0$ J$\cdot$mol$^{-1}\cdot$K^{-1}; The small value of $\Delta G^{\neq}$ (95.1 kJ$\cdot$mol^{-1} at 25°C) or $\Delta H^{\neq}$ suggests the relatively low potential barrier of the amine oxidation with **4** by the electron-transfer reaction from **2a–b** to **4** in Reaction (2c).

*3.3. Stereospecific oxidation of enantiomeric α-phenylethylamines (**2a** and **2b**) by chiral iron(III) porphyrins (**1a** and **1b**)*

The oxidation of *R*(+)-**2a** or *S*(−)-**2b** by **1a** or **1b** in benzene under N_2 at 25°C also proceeds in the biphasic fashion (Fig. 5), and the determined k_1^{obs} and k_2^{obs} values are listed in Table 2.

It is obvious from Table 2 that *S*(−)-**2b** is more easily oxidized by the present chiral iron(III) complex of **1a** or **1b** than *R*(+)-**2a**; Such a preferential coordination and reactivity of *S*(−)-**2b** toward **1a** or **1b** rather than *R*(+)-**2a** was observed in both the slow Reactions (2b) and (2c) as reflected by the enantiomer rate ratios (S/R in the k_1^{obs} and k_2^{obs} values). The relative values of $k_1^{obs}(S)/k_1^{obs}(R)$ and $k_2^{obs}(S)/k_2^{obs}(R)$, respectively, imply the following: (a) the chiral bis-ligated complex of $[Fe^{III}(S(-)\text{-}\mathbf{2b})_2T_{men}PP]^+Cl^-$ (*S,S*-**4a**) or $[Fe^{III}(S(-)\text{-}\mathbf{2b})_2T_{boc\text{-}Ala}PP]^+Cl^-$ (*S,S*-**4b**) is predominantly formed via Reaction (2a–b) more than $[Fe^{III}(R(+)\text{-}\mathbf{2a})_2T_{men}PP]^+Cl^-$ (*R,R*-**4a**) or $[Fe^{III}(R(+)\text{-}\mathbf{2a})_2T_{boc\text{-}Ala}PP]^+Cl^-$ (*R,R*-**4b**), and (b) the present amine oxidations prevail in the stereoselective Reaction (2c) between *S,S*-**4a** (or *S,S*-**4b**) and *S*(−)-**2b** rather than between *R,R*-**4a** (or *R,R*-**4b**) and *R*(+)-**2a** (see Fig. 6).

Therefore, the chiral portion of (−)-menthyl (in **1a**) or L(−)-alanine moiety (in **1b**) predominated the ligation or oxidative interaction of *S*(−)-**2b** rather than *R*(+)-**2a**. The linear relation expressed by Eq. 3c was also recognized for the stereoselective oxidation of **2a** or **2b** by the chiral **1a–b** complexes (for example, see Fig. 7), and k_1 and k_{-1}/k_2 values

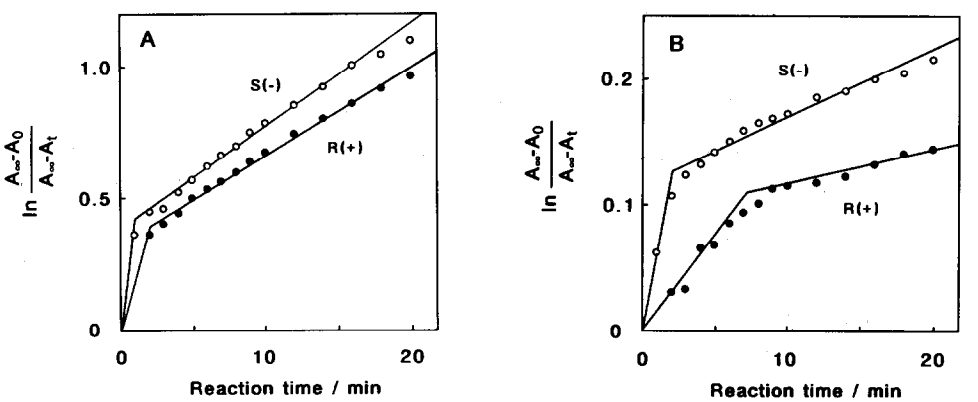

Fig. 5. Pseudo-first-order plots for the stereoselective oxidation of **2a** (or **2b**), (A) by **1a** or (B) by **1b**, in benzene at 25°C.

Table 2
Pseudo-first-order rate constants for the oxidation of **2a**(or **2b**) by **1a–b**[a]

[**2a**(or **2b**)]$_0$	$10^4 k_2^{obs}/s^{-1}$					
	1a			**1b**		
mol·dm^{-3}	*R*-**2a**	*S*-**2b**	*S*/*R*	*R*-**2a**	*S*-**2b**	*S*/*R*
0.5	0.8	1.1	1.38	0.19	0.24	1.76
0.75	1.8	2.4	1.33	–	–	–
1.5	6.2	8.1	1.31	0.34	0.41	1.21
	(30.2	37.5	1.24)[b]	–	–	–
2.5	–	–	–	0.52	0.59	1.13
				(2.18	2.93	1.34)[b]

[a] [**1a–b**] = 5.0–10^{-5} mol·dm^{-3} in benzene under N_2 at 25°C.
[b] The values in parentheses are corresponding to $10^4 k_1^{obs}$.

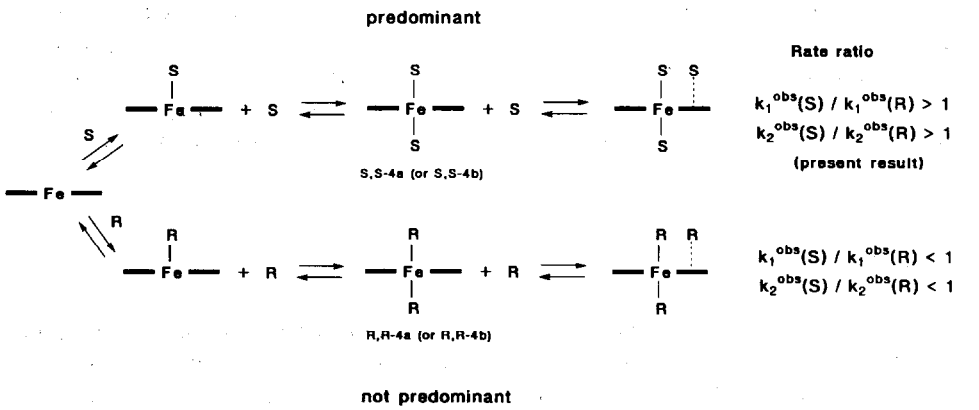

Fig. 6. Prevailed molecular recognition in Reaction 2c.

for the reaction of **1a** and **2a** (or **2b**) were determined to be $k_1(S) = 2.3 \times 10^{-3}$ mol^{-1}·dm^3·s^{-1}, $k_1(R) = 2.2 \times 10^{-3}$ mol^{-1}·dm^3·s^{-1}, $k_{-1}(S)/k_2(S) = 4.7$ mol·dm^{-3}, and $k_{-1}(R)/k_2(R) = 6.2$ mol·dm^{-3}. Among the rate ratios of $k_1(S)/k_1(R) = 1.05$ and $k_2(S)/k_2(R) = 1.32$, the latter falls in the range of the enantiomer rate ratios of k_1^{obs} and k_2^{obs} for *R*-**2a** and *S*-**2b**, indicating the predominant ligation of *S*-**2b** to **1a** rather than that of *R*-**2a** to **1a**.

It is clear from Tables 1 and 2 that the activities of the present iron(III) complexes follow the order of **1a** > **1c** > **1b**. The lowest activity of **1b** for the amine oxidation is probably due to the steric hindrance of the axial $\alpha,\alpha,\alpha,\alpha$-type *t*-butyloxycarbonyl-L(−)-alanine moiety against both the ligation (in Reaction (2a–b)) and the interaction (in Reaction (2c)) of **2a** (or **2b**) to **1b**. The extent of the stereoselection by **1b** was found to be larger in the k_1^{obs} step rather than in the k_2^{obs} one; this presumably implies that the k_1^{obs} (or k_2^{obs}) step is corresponding to the high (or low, respectively,) extent of the molecular recognition by

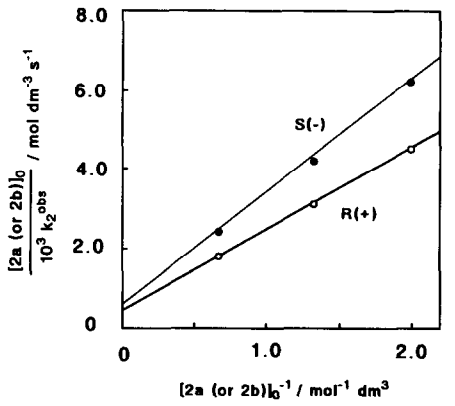

Fig. 7. Linear kinetic relation between [**2a** (or **2b**)]$_0/k_2^{obs}$ and [**2a** (or **2b**)]$_0^{-1}$ in the case of **1a**.

the chiral alanine part of **1b** in the interaction step of Reaction (2c) (or the second ligation step of Reaction (2b)). In this respect, the higher activity of **1a** as compared with **1c** may be ascribed to the facilitated interaction between **2b** and *S,S*-**4a** in the slow Reactions (2b and 2c), and the extent of the stereoselection by **1a** was larger in the k_2^{obs} step than in the k_1^{obs} one. Then, the chiral (−)-menthyl part in the equatorial portion of **1a** plays a predominant role in the molecular recognition in the second ligation step for the formation of the bis-ligated *S,S* (or *R,R*)-**4a**.

4. Conclusion

The present chiral iron(III) porphyrin complexes (**1a** and **1b**) stereoselectively recognized the enantiomeric amines (**2a–b**) during the ligation or interaction step in Reaction (2b or 2c). The extent of the stereoselection, however, was dependent not only on the molecular structures of **1a–1b** but also on the two slow reaction steps of Reactions (2b–c) in which the rate-determining step might be changed by the reactants as reflected in the rate-determining Reaction (2c) between **4** and **2a–b** [8], or in the rate-determining Reaction (2b) between **4′** and **2a–b** [7].

References

[1] T.L. Poulos, B.C. Finzel and A.J. Howard, J. Mol. Biol., 195 (1987) 687; S.S. Boddupalli, C.A. Hasemann, K.G. Ravichandran, J. Lu, E.J. Goldsmith, J. Deisenhofer and J.A. Peterson, Proc. Natl. Acad. Sci. USA, 89 (1992) 5567; N.C. Gerber and S.G. Sligar, J. Am. Chem. Soc., 114 (1992) 8742.

[2] H. Imai, S. Nakagawa and E. Kyuno, J. Am. Chem. Soc., 114 (1992) 6719.

[3] M.P. Byfield and J.M. Pratt, J. Chem. Soc., Chem. Commun., (1992) 214; E. Mikros, F. Gaudemer and A. Gaudemer, Inorg. Chem., 30 (1991) 1806; M. Tabata and A. Shimada, Bull. Chem. Soc. Jpn., 63 (1990) 672.

[4] Y. Aoyama, T. Uzawa, K. Saita, Y. Tanaka, H. Toi, H. Ogoshi and Y. Okamoto, Tetrahedron Lett., 29 (1988) 5271.

[5] P.L. Maux, H. Bahri and G. Simonneaux, J. Chem. Soc., Chem. Commun., (1991) 1350.
[6] J.T. Groves and R.S. Myers, J. Am. Chem. Soc., 105 (1983) 5791; J.T. Groves and P. Viski, J. Org. Chem., 55 (1990) 3628; D. Mansuy, P. Battioni, J.P. Renaud and P. Guerin, J. Chem. Soc., Chem. Commun., (1985) 155; J.P. Collman, X. Zhang, R.T. Hembre and J.I. Brauman, J. Am. Chem. Soc., 112 (1990) 5356; J.P. Collman, V.J. Lee, X. Zhang, J.A. Ibers and J.I. Brauman, J. Am. Chem. Soc., 115 (1993) 3834; S. O'Malley and T. Kodadek, J. Am. Chem. Soc., 111 (1989) 9116; S. O'Malley and T. Kodadek, Tetrahedron Lett., 32 (1991) 2445; K.C. Brown and T. Kodadek, J. Am. Chem. Soc., 114 (1992) 8336; Y. Naruta, F. Tani and K. Maruyama, J. Chem. Soc., Chem. Commun., (1990) 1378; Y. Naruta, F. Tani, N. Ishihara and K. Maruyama, J. Am. Chem. Soc., 113 (1991) 6865; K. Konishi, K. Oda, K. Nishida, T. Aida and S. Inoue, J. Am. Chem. Soc., 114 (1992) 1313; L. Chiang, K. Konishi, T. Aida and S. Inoue, J. Chem. Soc., Chem. Commun., (1992) 254.
[7] C.E. Castro, M. Jamin, W. Yokoyama and R. Wade, J. Am. Chem. Soc., 108 (1986) 4179.
[8] J.D. Gaudio and G.N. La Mar, J. Am. Chem. Soc., 100 (1978) 1112.
[9] A.D. Adler, F.R. Longo, J.D. Finarelli, J. Goldmacher, J. Assour and L. Korsakoff, J. Org. Chem., 32 (1967) 476.
[10] A.D. Adler, F.R. Longo, F. Kampas and J. Kim, J. Inorg. Nucl. Chem., 32 (1970) 2443.
[11] K. Ohkubo, T. Sagawa and H. Ishida, Inorg. Chem., 31 (1992) 2682.
[12] M. Momenteau, Biochim. Biophys. Acta, 304 (1973) 814; C.E. Castro and S.E. Anderson, Inorg. Chem., 24 (1985) 1113.
[13] H. Scheer and J.J. Katz, in K.M. Smith (Ed.), Porphyrins and Metalloporphyrins, Elsevier, Amsterdam, 1975, Chap. 10.